Journal of Robotics and Control (JRC)
Volume 4, Issue 4, 2023
ISSN: 2715-5072, DOI: 10.18196/jrc.v4i4.18429

Smart Robotic Exoskeleton: Constructing Using 3D Printer Technique for Ankle-Foot Rehabilitation

Rafal Khalid Salih [1*], Wajdi Sadik Aboud [2]
[1, 2] Prosthetics and Orthotics Engineering Department, Al-Nahrain University, Baghdad, Iraq
Email: [1] raffalkhalid95@gmail.com, [2] wajdisadik@gmail.com
*Corresponding Author

Abstract—**Patients with spinal cord injury (SCI), stroke, and coronavirus patients must undergo a rehabilitation process involving programmed exercises to regain their ability to perform activities of daily living (ADL). This study focuses on the rehabilitation of the foot-ankle joint to restore ADL through the design and implementation of a rehabilitation exoskeleton with three degrees of freedom (abduction/adduction, inversion/eversion, and plantarflexion/dorsiflexion movements). increase the patients cause worker fatigue, emotional exhaustion, a lack of motivation, and feelings of frustration, all contributing to a decrease in work efficacy and productivity. The robotic exoskeleton was developed to overcome this limitation and support the medical rehabilitation section. The main goal of this study is to develop a portable exoskeleton that is comfortable, lightweight, and has a range of motion (ROM) compatible with human anatomy to ensure that movements outside of this range are minimized, the anthropometric parameters of a typical human lower foot have been considered. In addition, it's a home-based rehabilitation device which means the exoskeleton can be used in any environment due to its lightweight and small size to accelerate the rehabilitation process and increase patient comfort. The proposed autonomous exoskeleton structure is designed in Solid Works and constructed with polylactic acid (PLA) plastic, the reason PLA was chosen is its lightweight, available, stiff material, and low cost, using 3D printing technology the exoskeleton was manufacturing. Electromyography (EMG) and angle data were extracted using EMG MyoWare and gyroscope sensors, respectively, to control the exoskeleton. It was evaluated on its own then with 2 normal subjects and 17 patients with stroke, spinal cord injury (SCI), and coronavirus. The limitation that has been faced was that the sessions were limited due to the limited time provided for the study. According to the improvement rate, the exoskeleton has a significant impact on regaining muscle activity and improving the range of motion of foot-ankle joints for the three types of patients. The rate of improvement was 300%, 94%, and 133.3% for coronavirus, SCI, and stoke respectively. These results demonstrate that this exoskeleton can be utilized for physiotherapy exercises.**

Keywords—CAD; Robotic Exoskeleton; Rehabilitation; FDM; Active; Passive; EMG.

I. INTRODUCTION

Due to stroke, musculoskeletal disorders, spinal cord injuries, and coronavirus, many people cannot walk. These individuals have lost function in their lower limbs (hip, knee, ankle, foot, or a combination). Therefore, their treatment must be enhanced by employing modern rehabilitation techniques and robotic exoskeleton rehabilitation is one of them [1]-[4].

For stroke patients in the industrialized globe, the annual incidence of stroke is approximately 180 per 100,000 inhabitants [5]. Three months after a stroke, one-third of the survivors are still alive. Approximately 80% of ambulatory patients are still dependent on a wheelchair, and their gait speed and endurance are substantially reduced [6]. Consequently, the restoration and enhancement of walking functions is a top priority for the desired social and occupational reintegration. Stroke patients are the individuals that benefit most from these exoskeletons. Stroke is a fatal disease that has recently shown accelerated growth and high death.

Spinal cord injury (SCI) patients who suffer from paralysis can use these exoskeletons to enhance recovery [7]-[9]. The SCI around the worldwide incidence ranges between 250,000 and 500,000, The treatment of spinal cord injuries requires inter-professional collaboration. The acute phase requires professional emergency treatment, whereas the chronic phase is frequently accompanied by long-term complications, necessitating long-term rehabilitation, and nursing. For effective use of medical resources and the development of targeted preventive and nursing measures [10][11].

People with strokes experience hemiplegia paralysis, which means that half of the body is paralyzed, either on the left or right side. While the SCI has paraplegia paralysis, this indicates that the lower limb is entirely paralyzed.

Exoskeletons are external devices attached to the human body that enable their users to perform at a level they cannot achieve on their own. Passive (P) or active (A) exercises are rehabilitation exercises. In passive exercises, therapists or the robot actively assist the subjects in moving the affected parts. In contrast, the subjects must exert effort to move the affected parts independently during active exercises [12]-[15]. The therapists become increasingly stressed as the number of patients increases, and as the number of patients increases, the number of therapists may decrease. Furthermore, the rehabilitation process becomes less effective, and patients become less active. This will hurt the individual's ability to regain functional independence and daily activities. The introduction of such rehabilitation devices has the potential to solve the aforementioned issues in a significant manner, thereby enhancing the rehabilitation program's effectiveness. Several studies have demonstrated a correlation between restoring and enhancing motor skills and demanding and repetitive functional tasks [16][17].

Significant progress has been made in rehabilitation robotics. However, obstacles continue to stand in the way of these developments and the full realization of the main objective (restoring bodily functions). The hardware's system and control mechanism may be partially responsible for these limitations. limitations in range of motion due to the hardware's implementation, complexity, cost, discomfort, weight, incompatibility with the human, mechanical structure, lack of safety features, and inefficient power transmission methods.

Due to the importance of exoskeleton robotics in medical rehabilitation today, intensive and brief studies have been conducted over the past few years to learn about the devices, their characteristics, and their drawbacks. Additionally, studies have been conducted to compare prices, weights, effectiveness, power sources, and control systems, some these studies [18]-[21]. Some studies were toward the materials, actuations, and manufacturing methods [22]. While some studies were to know the last trends in the developments of 3D printing legs exoskeletons [23]-[25]. While some studies toward the control strategies of the lower limb exoskeletons [26].

Kalra et al. [28] wrote an analysis of the use of robotics in healthcare. They serve as a rehabilitation aid for the upper and lower limbs, The use of robotics in healthcare dates back to the 1960s for surgery and the 1990s for rehabilitation, and it has since evolved into a variety of inexpensive, accessible new technologies with diverse control systems, varying degrees of freedom, and distinct working methods.

In 2021, Dong et al. [29] Developed a new ankle robotic system with three rehabilitation training strategies based on an admittance controller: patient-passive compliance exercise, isotonic exercise, and patient-active exercise, which take into account the patient's muscle strength and recovery stages, he parallel ankle rehabilitation robot features three degrees of rotation and two linear servo actuators and one servo motor.

In 2023, Qu et al. [30] presents a novel ankle rehabilitation hybrid mechanism that can accommodate the size requirements of various adult lower extremities. This model relates to three categories of ankle movement modes, without axis offset, and can account for ankle joint movement. The mechanism's inverse and forward position/kinematics results are analyzed utilizing the closed-loop vector method and the optimization of the particle groups algorithm. Also, there are more studies concerned with robotic devices and provided a great result for the users [31]-[38].

All patients must have access to rehabilitation devices through their presence in hospitals and rehabilitation centers. As a result of their bulky size or for other reasons, medical devices are frequently immobile in hospitals. These restrictions impose a significant burden on patients in addition to the high cost and they do not reside close to any hospitals or rehabilitation centers.

This study seeks to remedy these problems by overcoming limitations in current robotic exoskeleton designs and enhancing device specifications to make them more suitable for patients regardless of age, gender, or weight. The foot-plate was designed according to anthropometric data of the human body of males and females respectively, which means that the foot length was calculated to suit all the foot lengths of various patients. The weight of the foot was included and calculated according to anthropometric data meaning all the various foot weights the exoskeleton can handle.

The presented exoskeleton allows for three degrees of freedom (dorsiflexion/plantar-flexion, adduction/ abduction, and inversion/eversion) for use in ankle and foot rehabilitation. The performance and range of motion of such a device have been evaluated and analyzed; the device was assessed by itself and in cooperation with normal subjects. Utilizing Solid Works software and 3D printer technology, both of which can work with various materials, including plastic, the device's high-precision final construction is possible. The PLA material has been used to build the proposed exoskeleton, and its biodegradability, the primary advantages of PLA for fused deposition modeling (FDM) printing are its low glass transition temperature and absence of harmful gases during melting, allowing it to be printed without an exhaust system. Also, its affordability and lightweight [39]-[41].

II. ANATOMY OF THE ANKLE JOINT

The anatomy of the ankle joint complex shows that it is not just a simple hinge joint but that of multi-axial motions occurring simultaneously to facilitate human gait. The human foot's anatomy and kinematics are explained. The human ankle consists of multiple joints. Talus is the middle bone. The cuboid and navicular bones surround it. The upper portion of the talus articulates with the tibia and fibula portions of the shinbone. This is the UAJ, the top joint of the ankle. It facilitates plantarflexion and rotational dorsiflexion. For rotation of the ankle joint in three-dimensional space, the movements of the fore bones are firmly connected. This allows the inversion/eversion rotation. Fig. 1 illustrated the ankle joint movements. There are a lot of studies that concerned with ankle-foot anatomy studies [42]-[56], and to know the mechanism of the ankle-foot movements in order to create a robotic exoskeleton suitable to the ankle movements a wide spread of studies have been done [57]-[62].

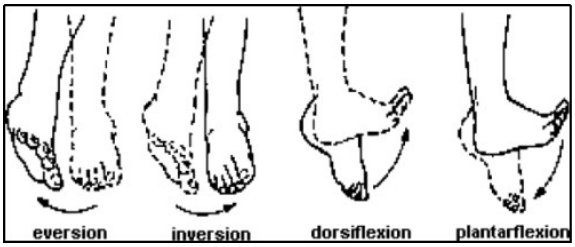

Fig. 1. Main foot rotations around the two axes of the ankle [42]

III. DESIGN CONSIDERATION

Because of their proximity to the human body, rehabilitation devices have stringent structural requirements that must be met. Since the ankle joint and foot provide movements around an axis that is not fixed, the mechanical structure must be built in such a way that it is compatible with the anatomical form of the human body. This allows the

device to be adjusted to accommodate patients of varying heights, weights, and ages, making the rehabilitation process more inclusive by taking the anthropometric data of leg-foot length and weight and designing the exoskeleton according to it to fit all leg-foot length and weight. The foot length and weight were calculated before the exoskeleton manufacturing, through the anthropometric data as illustrated in Table I. Beyond the device's safety and comfort features, the normal range of motion and the speed at which it works when dealing with the case of a patient in rehabilitation are among the most important factors to consider. By analyzing the device's ROM by the Gyroscope sensor with its own, the safety of the device was evaluated, indicating the maximum degree that the exoskeleton can reach, to prevent the exoskeleton from accessing the normal ROM of the human body, the ROM of the exoskeleton is two degrees less than that of the human body, the ROM of normal people and exoskeleton illustrated in Table II and Table III.

The most important consideration is the comfort of the patients that used the exoskeleton, in this study an external device is worn in the patient's leg before the foot insertion in the exoskeleton to increase the comfort and safety of the patient's leg as illustrated in Fig. 18.

TABLE I. LENGTH AND WEIGHT OF LEG AND FOOT SEGMENTS [63]

Segment	Variables	Female	Male
Leg	*Length*	25.70	24.70
	weight	5.35	4.75
Foot	*Length*	4.25	4.25
	weight	1.33	1.43
Length and weight of segment are (%) of human body height			

The weight and length of the human body are known, the maximum body weight that was reached in this study is 95Kg,

Leg weight= 95*9.81*4.75%=44.267 N

Foot weight=95*9.81*1.43%=13.326 N

By collecting the weight of the foot and leg, the results are 57.593 N, which is less than the weight that the exoskeleton can handle which is 60 N as illustrated in the ANSYS section. The applied force in ANSYS is illustrated in Fig. 2. Fig. 3 Illustrated study methodology.

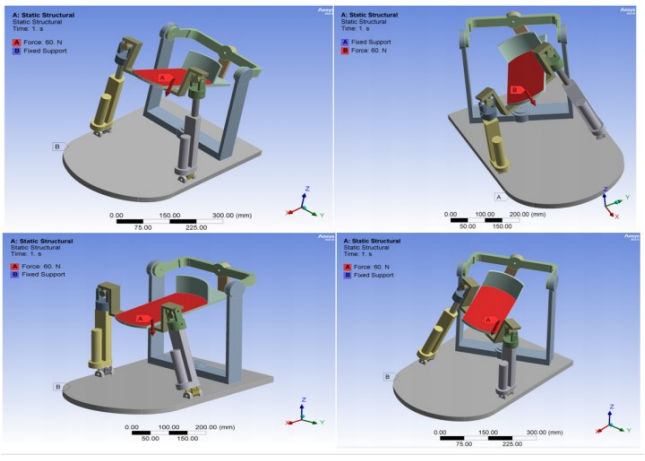

Fig. 2. The applied force in ANSYS

TABLE II. NORMAL HUMAN ROM [63]

Motion direction	ROM (degree)
Dorsiflexion	20.3–29.8
Plantarflexion	37.6–45.8
Inversion	14.5–22.0
Eversion	10.0–17.0
Abduction	15.4–25.9
Adduction	22.0–36.0

TABLE III. THE EXOSKELETON ROM

Motion direction	ROM (Degree)
Dorsi-Flexion	19.0-28.0
Planter-Flexion	36.2-44.4
Inversion	12.1-20.0
Eversion	8.0-15.0
Abduction	14.1-24.0
Adduction	20.0-34.0

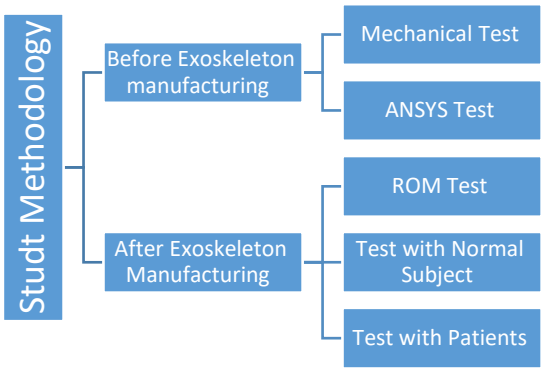

Fig. 3. Study methodology

IV. MECHANICAL DESIGN

The joints and links of the lower limb including the leg and foot weight and length were implemented based on the anthropometric data shown in Table I.

Implementation of the Ankle-Foot Exoskeleton was decomposing into major steps. First, a fixed base containing all exoskeleton components is fabricated. Next, a foot plate with one movement in the anatomical plane (dorsiflexion/plantarflexion) and two other movements (inversion/eversion, abduction/adduction) in the opposite plane are fabricated, resulting in an exoskeleton with three degrees of freedom 3DOF.

The CAD software Solid Works was used to create all of these components. The program's ease of use and flexibility in accommodating the designer's requests for changes to the implemented structure to decrease the margin of error and address any implementation issues were significant factors in the designer's decision to use this tool. In addition to the aforementioned capabilities, it is also capable of converting and storing the implemented mechanical structure in a format compatible with all types of 3D printers, thereby enabling the subsequent fabrication of each component using 3D printer technology. Fig. 4 shows the CAD model of exoskeleton parts. The proposed exoskeleton is printed on an Any cubic Mega-S 3D printer, as shown in Fig. 5 and Fig. 6 the printed part of the exoskeleton and the assembly of it.

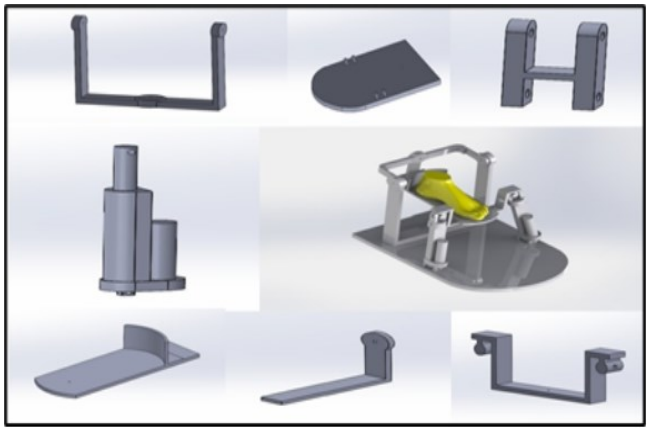

Fig. 4. CAD Model of the Exoskeleton Parts and its Assembly in Solid Work

Fig. 5. Printed parts of the exoskeleton

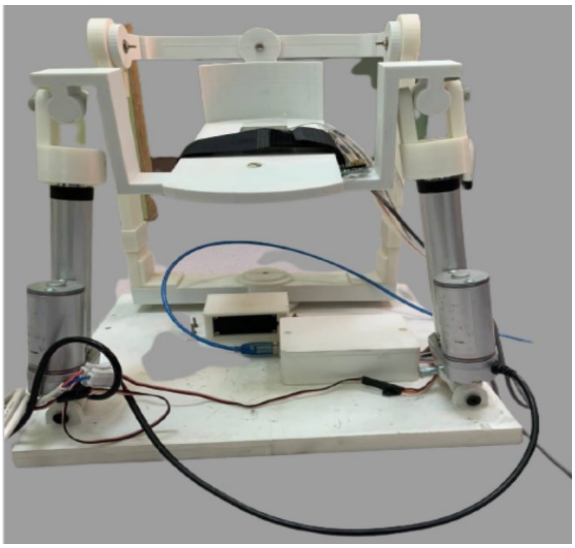

Fig. 6. Ankle-Foot Exoskeleton

The main components of the proposed ankle-foot exoskeleton are:

1. Myo-Ware 2.0 Muscle Sensor Module
2. Gyroscope Sensor.
3. Force Sensing Resistor 406
4. Two push bottoms
5. Two Arduino Uno
6. Arduino Joystick
7. DC motor Driver L298
8. Two linear actuators 100mm
9. Servo motor 50 kg.cm
10. Liquid crystal LCD 4x20.

Fig. 7 illustrates the electrical components assembly while Fig. 8 illustrates the operation of the control system.

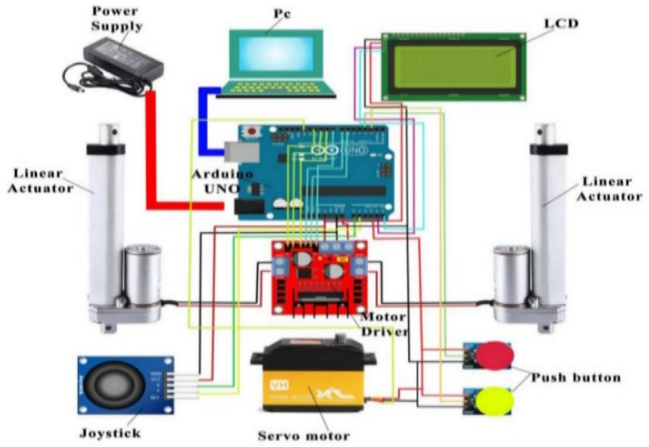

Fig. 7. The electrical component of the ankle-foot exoskeleton

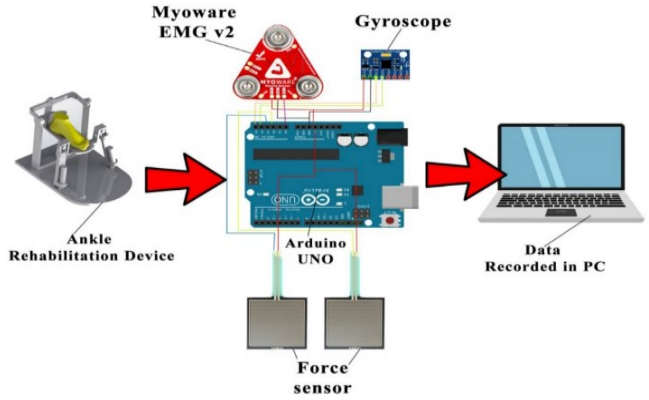

Fig. 8. Operation of a control system

V. FORWARD KINEMATIC

Kinematics is the branch of mechanics that describes the motion of bodies and fluids without reference to the forces that cause the motion. The purpose of kinematics is to describe the motion of the manipulator without regard to the forces and torques that cause the motion. Therefore, the kinematic description is geometric. First, we consider the forward kinematics problem, which involves determining the position and orientation of the end-effector given the joint variable values of the robot [64]-[66].

Kinematics is the study of the motion of multi-body, jointed mechanisms such as robots and, more specifically, exoskeletons. Kinematics is concerned with the analysis of the motion of each robot link in relation to a reference frame, and it involves the following steps:

- An analytical description of motion as a function of time.
- The nonlinear relationship between the position and orientation of the robot's end-effector and its configuration.

Usually, homogeneous transformation matrices are utilized for robot kinematics analysis. The relative motion of links around a joint in multilink mechanisms with joints, such as robots, can be simply described by homogeneous transformation matrices. The transformation between successive coordinate systems takes the kinematics of robot joints into account. The joints of a specific robot are numbered from 1 to n, beginning with the base joint and

ending with the end-effector. Then, the subsequent steps are required:

- Establish the base coordinate system OX0Y0Z0 with Z0 lying on the axis of motion of joint 1.
- Establish the joint axis by aligning Zi with the axis of motion of joint i + 1.
- Establish the rest joint axis.

Serial manipulator kinematics can be used to approximate foot kinematics. Employing Denavit Hartenberg-style homogeneous matrix transformations, abbreviated DH. Fig. 9 displays the assigned relative frames Oi between the moving links in the foot-ankle exoskeleton. Table IV shows the values of the D-H parameters of the exoskeleton. The transformation matrix from Oi+1 into Oi is denoted by the notation T_i^{i+1} (1-1) in equation (1) [67][68].

$$T_i^{i+1} = \begin{bmatrix} C(\theta i) & -C(\alpha i)S(\theta i) & S(\alpha i)S(\theta i) & aiC(\alpha i) \\ S(\theta i) & C(\alpha i)C(\theta i) & -S(\alpha i)C(\theta i) & aiS(\alpha i) \\ 0 & S(\alpha i) & C(\alpha i) & di \\ 0 & 0 & 0 & 1 \end{bmatrix} \quad (1)$$

where The relation states the transformation matrix from the final coordinate system to the initial coordinate system (2).

$$T_3^0 = T_1^0 T_2^1 T_3^2 \quad (2)$$

There are two frames located at the ankle:

- The base frame dorsiflexion–plantarflexion, X0Y0Z0
- inversion–eversion, X1Y1Z1.
- The end-effector is placed at the tip of the longest toe, X3Y3Z3.

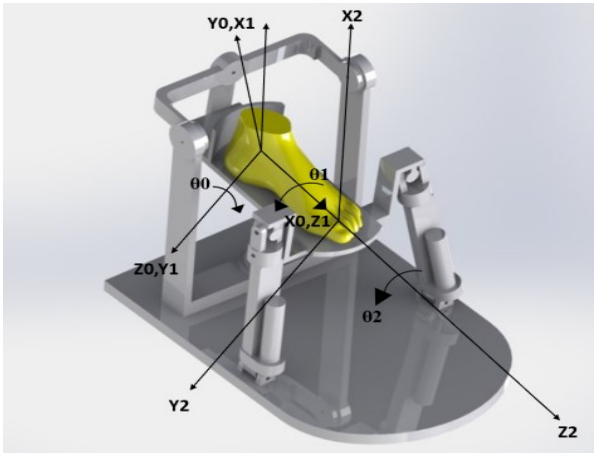

Fig. 9. Ankle-Foot Frame

TABLE IV. D-H PARAMETER OF ANKLE JOINT

Joint	ai	αi	di	θi
Ankle	0	0	0	θ1
Ankle (0→1)	0	π/2	0	θ2
Toe (1 →2)	L1	0	0	θ3

The angles θ_1 (dorsiflexion/plantarflexion) and θ_2 (inversion/eversion) are the model's independent variables, whereas θ_3 is constant. The foot is considered to be in the zero configuration of the equivalent serial manipulator when it is in the upright standing position. Substituting the DH parameters from Table II in equation (1) the result is shown in equation (3).

$$T_3^0 = \begin{bmatrix} c123 + s123 & c12s3 - s12c3 & 0 & l1 \\ s12c3 - c12s3 & s123 - c123 & 0 & 0 \\ 0 & 0 & 1 & 0 \\ 0 & 0 & 0 & 1 \end{bmatrix} \quad (3)$$

where $s1$, $c1$, $s2$, $c2$, $s12$, $c12$, $s13$, $c13$, and $c123$ referred to $sin\theta1$, $cos\theta1$, $sin\theta2$, $cos\theta2$, $sin(\theta1+\theta2)$, $cos(\theta1+\theta2)$, $sin(\theta1+\theta3)$, $cos(\theta1+\theta3)$, and $cos\ (\theta1+\theta2+\theta3)$ respectively. The 3x3 upper-left partitioned matrix of equation (3) represents the orientation of the joint with respect to the base frame while the upper-right 3x1 partitioned matrix represents the position vector. It has been cleared that the position vector (Pi) of all exoskeleton joints (i) with respect to the joint (i-1) is equal to zero.

VI. BEFORE EXOSKELETON MANUFACTURING PROCESS

This stage includes the exoskeleton materials selection and test. The test includes the tensile test and the tensile test results used in ANSYS as a boundary condition, PLA material is selected as the appropriate material due to its significant properties and cost. The mechanical tests for PLA material were done to find the PLA mechanical properties. The PLA specimen's dimension according to ASTM standard type I is illustrated in Fig. 10 While the PLA specimens of the tensile test before and after fracture are illustrated in Fig. 11. The results of mechanical tests are shown in Table V. The ANSYS software performed continuously to improve the design and choose the appropriate thickness for even the smallest sections of the device to ensure the greatest resistance the device can withstand during use and the greatest weight the robot can support. FEA is used to evaluate the device's reliability, stress distribution, and potential deformation to predict the stress and deformation under foot and limb load. Then the exoskeleton components were constructed. All of the exoskeleton's components were built and configured using the additive technique known as 3D printing, which is a method for creating virtually any form of computer-aided design (CAD) using thermoplastic materials such as polylactic acid (PLA). The PLA material is suitable for withstanding the aforementioned environmental properties and is also inexpensive and lightweight [69]-[71]. Fig. 4 shows the CAD data of the exoskeleton that has been added to the 3-D printer. A large-scale 3D printer from Any Cubic was employed in this study as seen in Fig. 12 The printer's dimensions are 300*300*305 mm, and it has a 350W power source that can produce temperatures of up to 260 C for the extruder and 100 C for the construction plate. The printer settings are managed by the Cure slicer, which produces G-code lines from the slicer program. Additionally, it is possible to directly alter the G-code, which is a great technique to get the required result. Although time-consuming, it is effective.

The extruder temperature was set for the experiment at around 210 °C, depending on the qualities of the material. Based on several printing efforts, the building plate temperature has also been shown to be a sensitive 3D printing parameter, and PLA works best at 60 °C. The printing speed was 45 mm/s, and the nozzle diameter was 0.4. The height between layers was 0.15 for gloves and 0.2 for mold, the print resolution was (0.2–0.15), the layer height was (0.2), and the

total time to print all parts was approximately 62 hours. The exoskeleton parts are printed, and each part was printed alone. Following the 3-D printing, the assembly process was done by screw.

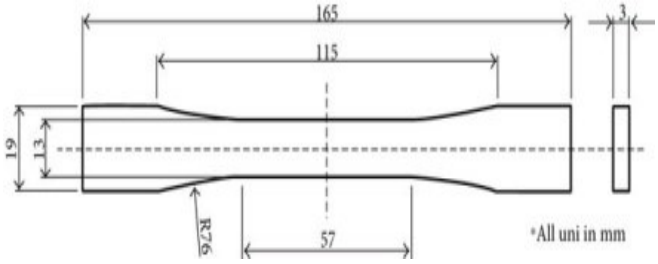

Fig. 10. Dimensions of tensile test specimens

Fig. 11. Tensile Test Specimens before and after a fracture

TABLE V. TENSILE TEST RESULTS

Number of samples	σ_b max (MPa)	E flexural (GPa)	Max.Load (N)	Stress Bending (Mpa)
Sample 1	82	1.5	140	-
Sample 2	94	3	160	76
Sample 3	82	3	140	70

Fig. 12. Any Cubic printer

VII. ANSYS ANALYSIS

A finite element analysis (FEA) was performed on the most critical parts to identify potential load failures. The mechanical structure was modified to accommodate the anticipated maximum loads. All exoskeleton components were subjected to FEA to determine stresses, deformation, and safety factors. The loads applied to exoskeleton components were distributed across their respective areas. The load applied is 60 N in Fig. 2, and the safety factors of all movements are shown in Fig. 13. The result of the mechanical test shows that the maximum yield stress is 54 MPa, and the maximum Von-Mises stresses values are 34.6 MPa for Inversion, 33.3 MPa for Eversion, 26.7 MPa for Dorsiflexion and finally 22.9 MPa for Plantarflexion. Therefore, the exoskeleton is safe during all movements because the Von Mises is less than the yield stress. Fig. 12 illustrates the stress analysis and the obtained safety factor. Fig. 14 the (Von-Mises) equivalent stress.

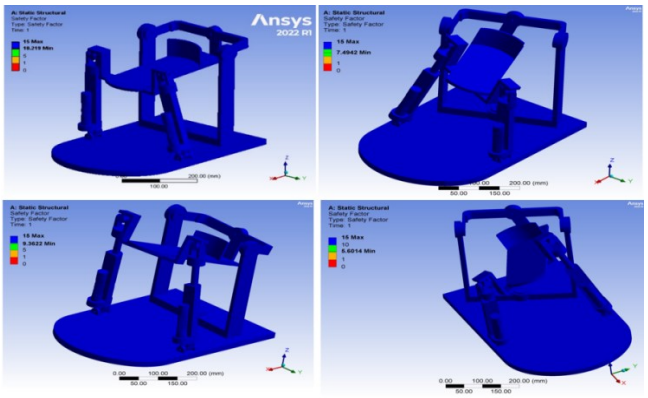

Fig. 13. ANSYS data, the factor of safety of inversion/eversion; abduction/adduction, and plantarflexion/dorsiflexion

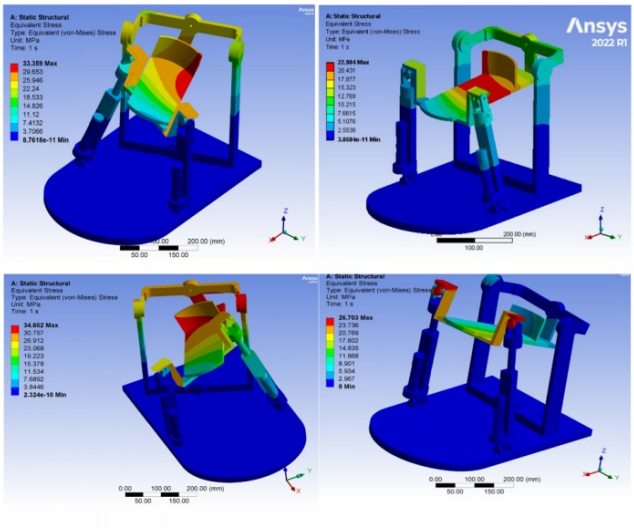

Fig. 14. Von-Mises Stress

Fused deposition molding (FDM) technology [72]-[77] was used to create the exoskeleton in its various parts. According to CAD software instructions, FDM works by melting a filament or metal wire from a coil to an extrusion nozzle, which can then move in horizontal and vertical directions according to instructions from computer-aided manufacturing (CAD) software. Parts printed in this manner have significantly more strength along the plane of printing than they would have been printed in the conventional direction, as each heating layer makes contact with the subsequent layer and is drawn with each other. As a new layer is printed, the previous one solidifies and cools.

VIII. ELECTRONIC DESIGN

The exoskeleton was pre-wired with electronic components such as a gyroscope sensor for angle measurement located at the exoskeleton's footplate (to pick up all three movements of the exoskeleton) and electromyography (EMG) sensor that is used to show the muscles activity. Also, the EMG sensor operates the active mode. And Arduino Uno controller; the motors and

gyroscope, EMG sensors were programmed to provide information emulating that of a normal human's range of motion and to evaluate this information, respectively.

The motors' control strategy is dependent on the angle data transmitted by the gyroscope sensor. In the absence of angle data from the patient, the exoskeleton will operate in passive mode; otherwise, it will switch to active mode. The Gyroscope and EMG connection with Arduino Uno is shown in Fig. 15 and Fig. 16 illustrates the FSR, Gyroscope and EMG sensors.

According to some studies that studied the EMG values of the normal people in several positions such as running, sitting. The EMG values for normal human body were between 200-350 mv [78]-[80].

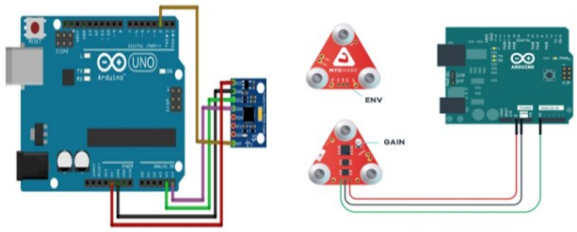

Fig. 15. The Gyroscope and EMG connection with Arduino Uno

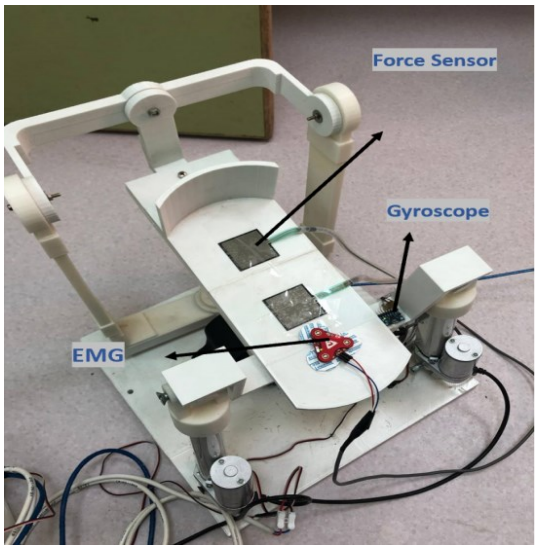

Fig. 16. FSR, Gyroscope, and EMG sensors

IX. AFTER EXOSKELETON MANUFACTURING PROCESS

This section includes the Exoskeleton Test, the ROM on its own, and two healthy subjects. After the test has been done successfully, the exoskeleton is finally applied to patients. The ROM is performed to ensure safety, comfort, capacity to carry and withstand heavy loads, and suitability for patients of all ages, sizes, and genders were also evaluated. This testing has been conducted to ensure that the exoskeleton can be used to rehabilitate patients and assist them in resuming their daily activities. Table III displays the exoskeleton's resulting range of motion. Fig. 17 depicts the ROM of the device on its own of the three movements. The exoskeleton mode of operation has two modes; the first mode is the passive mode which operates the exoskeleton via a Joystick without any intervention from the patient. The second mode is the active mode which operates via an EMG sensor. The sensor is put on the Gastrocnemius muscle and moves the device by muscle construction. Fig. 18 illustrates the whole Ankle-Foot exoskeleton assembly, mechanism, and components.

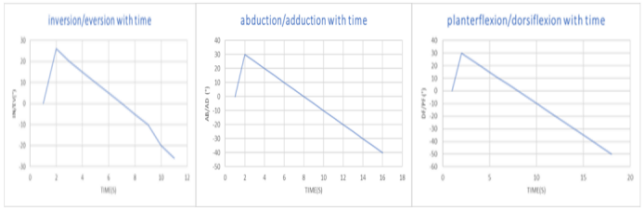

Fig. 17. Exoskeleton ROM of inversion/eversion; abduction/adduction and plantarflexion/dorsiflexion

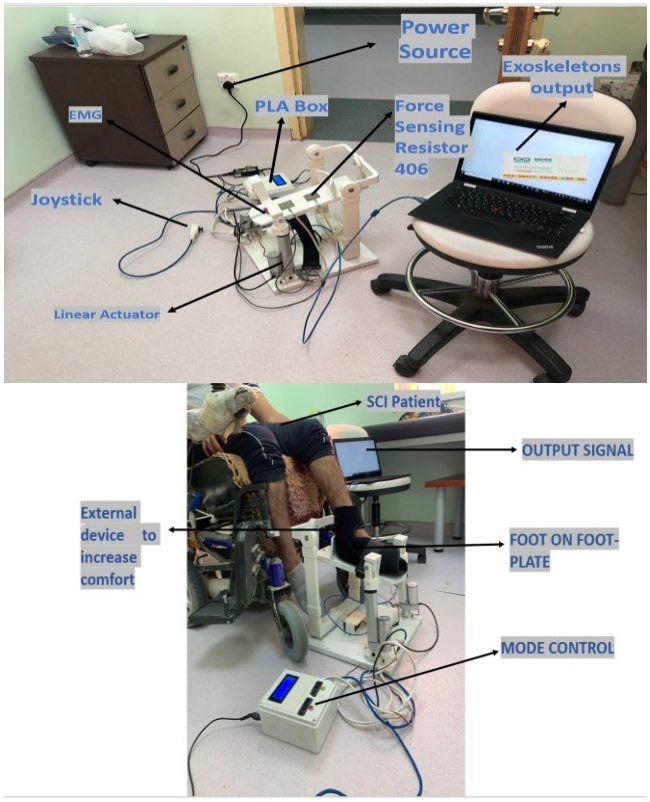

Fig. 18. Ankle-Foot Exoskeleton mechanism and components

Two healthy subjects and 17 paretic patients participated in experiments throughout the study. Nonetheless, the modes of operation were evaluated with each subject. The subjects' data are shown in Table VI. Before participating in experiments approved by the physiotherapy center of the Fallujah teaching hospital's Department of Physiotherapy, all healthy and sick subjects were informed of the experimental protocols and consented. In addition, precautions were taken to protect the subjects' privacy and the confidentiality of their personal information. All healthy subjects were able to perform full movements of the ankle joint. The rehabilitation lasts for two months (eight weeks, each week two sessions) the results are 16 sessions for each patient. In this study, three cases are tested which are as follows:

- 12 patients have strokes,
- Only one patient has coronavirus,
- 4 patients have spinal cord injury (SCI).

TABLE VI. PATIENTS' DATA

No.	Name	Sex	Age	Mass (Kg)	Type of Disease	Time since injury
1	J.H.	F*	66	57	Right stroke	2Y*
2	A.KH.	M*	53	90	Right stroke	13Y
3	T.M.	F	62	78	Left stroke	7M*
4	KH.J.	M	51	85	Left stroke	5M
5	S.J.	M	69	91	Left stroke	1Y
6	S.N.	M	27	66	Right stroke	2Y
7	S.KH	M	47	80	Left stroke	2Y
8	N.J.	M	59	75	Left stroke	3M
9	N.W.	M	51	70	Right stroke	3M
10	W.H.	F	10	40	Right stroke	3Y
11	Y.KH.	M	50	95	Right stroke	5M
12	N.H.	F	70	84	Left stroke	1M
13	A.H.	F	16	55	Corona	7M
14	A.M.	M	23	58	SCI	10Y
15	S.N.	M	30	90	SCI	Y
16	L.S.	M	35	86	SCI	1Y
17	Y.Y.	M	33	70	SCI	2Y

*F=Female, M=Male. *Y=Year, M=Month

The EMG signals of muscles are recorded for each patient, and the muscle improvements of stroke patients were so satisfied. As illustrated the sessions last for two months, which means 16 sessions. Fig. 22 to Fig. 24 illustrates the ROM progression during the 16th session for the stroke patients, SCI patients, and coronavirus patient. The first EMG muscles' reading of the stroke patients was between 75.11 - 95.04 mV, while in the last session was between 301.12 - 340.13 mV. Fig. 19 illustrates the EMG progression for gastrocnemius and anterior tibialis muscle during the first and last sessions.

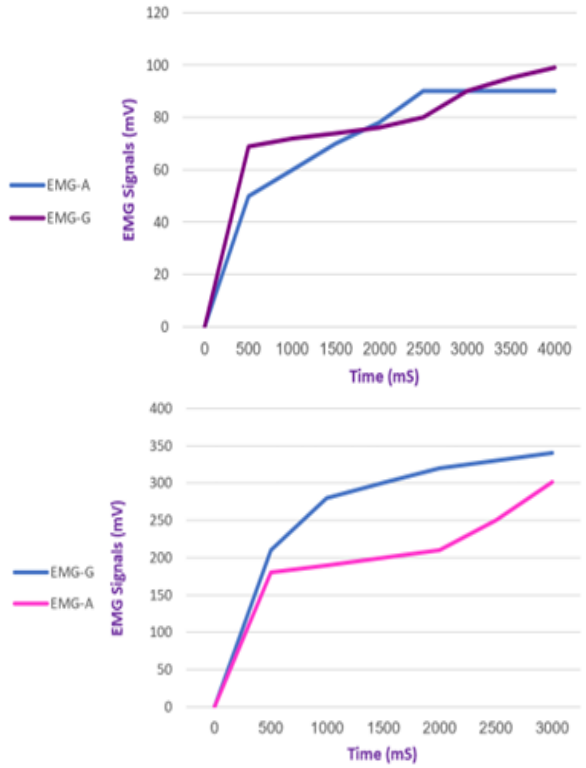

Fig. 19. EMG progression for gastrocnemius and anterior tibialis muscle during the first and last sessions

The first EMG muscles' reading of SCI patients was between 37.0 - 90.1 mV, while in the last session was between 66.19 - 175.00 mV. Fig. 20 illustrates the EMG progression for Left and Right leg muscles during the first and last sessions.

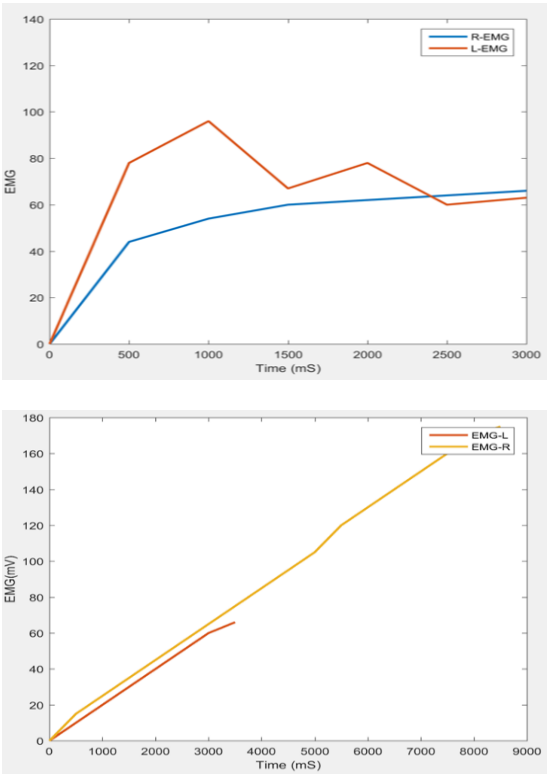

Fig. 20. EMG progression for Left and Right leg muscles during the first and last sessions

The first EMG muscles' reading of the corona-virus patient was between 78.50 - 90.00 mV, while in the last session was between 199.00 - 210.00 mV. Fig. 21 illustrates the EMG progression for Left and Right leg muscles during the first and last sessions.

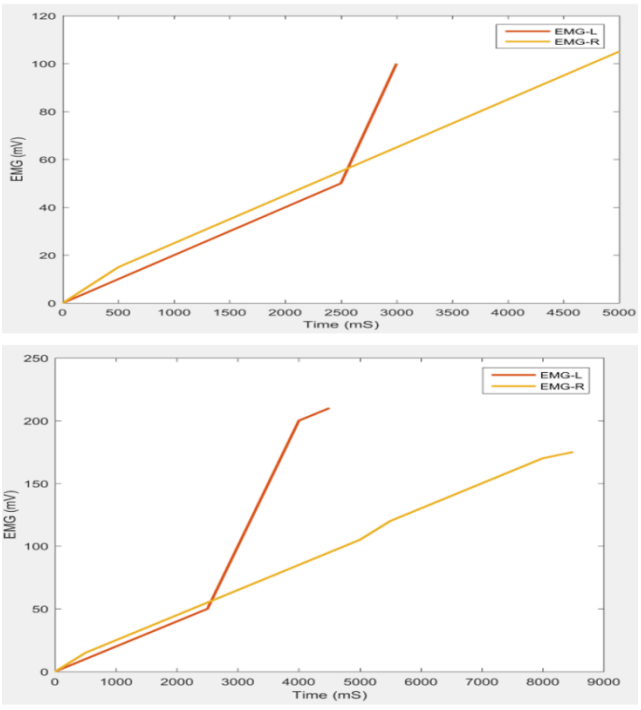

Fig. 21. The EMG progression for Left and Right leg muscles during the first and last sessions

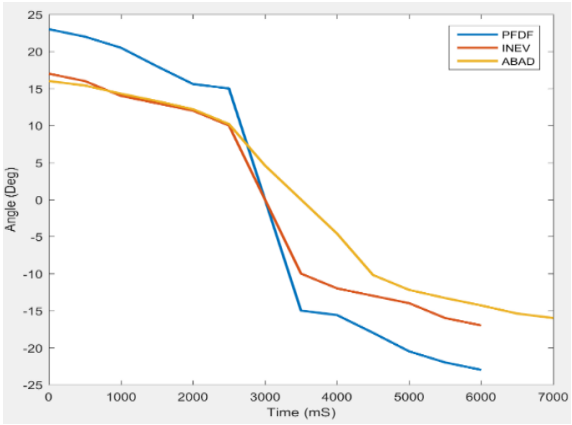

Fig. 22. ROM progression during the 16th session for the stroke patients

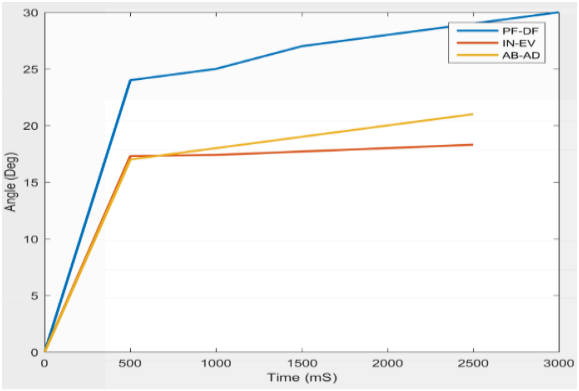

Fig. 23. ROM progression during the 16th session for the SCI patients

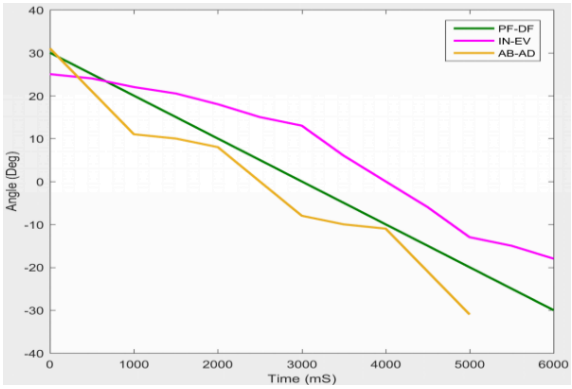

Fig. 24. ROM progression during the 16th session for the coronavirus patient

X. DISCUSSION

The study aims to implement and build a novel exoskeleton structure that rises above the constraints and challenges of previously proposed exoskeleton structures. The manufacturing process was treated with lightweight, inexpensive, and durable materials, resulting in a device with specific portability, affordability, and weight-independent use among multiple patients. This device was designed with three degrees of freedom to provide a comprehensive qualification of foot-ankle joints via a presetting training program with three modes of operation determined by the patient's rehabilitation progress and defect type. Because the exoskeleton was programmed to work primarily at lower velocities, its reflected range of motion is slightly less than half that of a normal human; however, the proposed velocities will be increased as the patient improves during the rehabilitation process via an increase in the voltage of the power supply.

XI. CONCLUSION

This study included foot anatomy to identify and design the principal foot and ankle movements. It also includes the mechanical test that is used as a boundary condition in the ANSYS program. The solid work (CAD) is then used to prepare the mechanical design for 3-D printing. The results indicated that the patients in this study had excellent outcomes. The material that has been used is PLA material due to its lightweight, strong, and economic. To improve the effectiveness of ankle rehabilitation, a lightweight robot with only three rotational degrees of freedom was developed. The proposed 3-DOF consists of an upper foot platform, two actuators for PF/DF motion, and one servomotor for IN/EV and AB/AD motion. The objective of this study was to develop an ankle exoskeleton with a minimum weight and cost. The total weight of the device is 4.500 kg, and it costs approximately $900. The aims of testing the system on healthy subjects are as follows: 1) to demonstrate that the system can modify the natural ankle joint with a high degree of repeatability; 2) to ensure the wearer's safety during experiments; and 3) to assess the accuracy of the ankle-foot rehabilitation operations mode. In addition to its small size, the EMG sensor aids in displaying the patient's progress via output readings. In addition to the role of repetitive evaluation, the entire therapy encouraged patients to enthusiastically complete their therapy. Also, this device allows the patients to exercise at home and during their available time. The results show the patient's progress through the EMG signals determining muscle strength. The proposed Ankle-foot exoskeleton shows promising results that would make the rehabilitation process faster and easier.

For future recommendations, for patients with two paralyzed legs, such as those with a spinal cord injury, a second foot plate can be added so that rehabilitation can be conducted simultaneously on both legs. Also, instead of a press button, the device can be remotely controlled via Bluetooth. Additionally, it can connect via a mobile app and be controlled via the app. incorporating Internet of Things (IoT) technology into the exoskeleton. The Internet of Things (IoT) refers to physical objects (or groups of such objects) with sensors, processing ability, software, and other technologies that connect and exchange data with other devices and systems over the Internet or another communications network, which means that the data of a home-based exoskeleton is collected and transmitted to the physiotherapy via the Internet.

ACKNOWLEDGMENT

The authors give acknowledge those whose contributions either influenced or were explicitly incorporated into this article. Special thanks to the Rehabilitation Center in Fallujah teaching hospital that supported me till the end of the work of this study.

REFERENCES

[1] A. G. Guggisberg, P. J. Koch, F. C. Hummel, and C. M. Buetefisch, "Brain networks and their relevance for stroke rehabilitation," in *Clinical Neurophysiology*, vol. 130, no. 7, pp. 1098–1124, 2019.

[2] C. M. Stinear, M. C. Smith, and W. D. Byblow, "Prediction tools for stroke rehabilitation," *Stroke*, vol. 50, no. 11, pp. 3314-3322, 2019.

[3] S. K. Lui and M. H. Nguyen, "Elderly Stroke Rehabilitation: Overcoming the Complications and Its Associated Challenges," in *Current Gerontology and Geriatrics Research*, vol. 2018, 2018.

[4] Y. Chen, K. T. Abel, J. T. Janecek, Y. Chen, K. Zheng, and S. C. Cramer, "Home-based technologies for stroke rehabilitation: A systematic review," *International journal of medical informatics*, vol. 123, pp. 11-22, 2019.

[5] A. Lloyd, K. Bannigan, T. Sugavanam, and J. Freeman, "Experiences of stroke survivors, their families and unpaid carers in goal setting within stroke rehabilitation: a systematic review of qualitative evidence," *JBI Evidence Synthesis*, vol. 16, no. 6, pp. 1418-1453, 2018.

[6] P. L. Kolominsky-Rabas and P. U. Heuschmann, "Incidence, etiology and long-term prognosis of stroke," *Fortschritte der Neurologie-psychiatrie*, vol. 70, no. 12, pp. 657-662, 2002.

[7] A. V. L. De Araújo, J. F. D. O. Neiva, C. B. D. M. Monteiro, and F. H. Magalhães, "Efficacy of Virtual Reality Rehabilitation after Spinal Cord Injury: A Systematic Review," in *BioMed Research International*, vol. 2019, 2019.

[8] M. Mekki, A. D. Delgado, A. Fry, D. Putrino, and V. Huang, "Robotic Rehabilitation and Spinal Cord Injury: a Narrative Review," in *Neurotherapeutics*, vol. 15, no. 3, pp. 604–617, 2018.

[9] L. Weber, N. H. Voldsgaard, N. J. Holm, L. H. Schou, F. Biering-Sørensen, and T. Møller, "Exploring the contextual transition from spinal cord injury rehabilitation to the home environment: a qualitative study," *Spinal Cord*, vol. 59, no. 3, pp. 336–346, 2021.

[10] F. Biering-Sørensen, "International Spinal Cord Injury Data Sets in clinical practice and research," *Archives of Physical Medicine and Rehabilitation*, vol. 103, no. 12, 2022.

[11] K. Nas, L. Yazmalar, V. Şah, A. Aydın, and K. Öneş, "Rehabilitation of spinal cord injuries," *World journal of orthopedics*, vol. 6, no. 1, p. 8, 2015.

[12] S. K. Hasan and A. K. Dhingra, "Biomechanical design and control of an eight DOF human lower extremity rehabilitation exoskeleton robot," *Results in Control and Optimization*, vol. 7, p. 100107, 2022.

[13] F. Molteni, G. Gasperini, G. Cannaviello, and E. Guanziroli, "Exoskeleton and end-effector robots for upper and lower limbs rehabilitation: narrative review," *PM&R*, vol. 10, no. 9, p. S174-S188, 2018.

[14] D. Shi, W. Zhang, W. Zhang, and X. Ding, "A review on lower limb rehabilitation exoskeleton robots," *Chinese Journal of Mechanical Engineering*, vol. 32, no. 1, pp. 1-11, 2019.

[15] J. Zhou, S. Yang, and Q. Xue, "Lower limb rehabilitation exoskeleton robot: A review," *Advances in Mechanical Engineering*, vol. 13, no. 4, 2021.

[16] T. C. Machado, A. A. Carregosa, M. S. Santos, N. M. S. Ribeiro, and A. Melo, "Efficacy of motor imagery additional to motor-based therapy in the recovery of motor function of the upper limb in post-stroke individuals: a systematic review," *Topics in stroke rehabilitation*, vol. 26, no. 7, pp. 548-553, 2019.

[17] R. Mane, T. Chouhan, and C. Guan, "BCI for stroke rehabilitation: motor and beyond," *Journal of neural engineering*, vol. 17, no. 4, 2020.

[18] Y. Ma, X. Wu, J. Yi, C. Wang, and C. Chen, "A review on human-exoskeleton coordination towards lower limb robotic exoskeleton systems," *Int. J. Robot. Autom*, vol. 34, no. 4, pp. 431-451, 2019.

[19] D. S. Pamungkas, W. Caesarendra, H. Soebakti, R. Analia, S. Susanto, "Overview: Types of lower limb exoskeletons," *Electronics*, vol. 8, no. 11, p. 1283, 2019.

[20] D. Pinto-Fernandez *et al*., "Performance Evaluation of Lower Limb Exoskeletons: A Systematic Review," in *IEEE Transactions on Neural Systems and Rehabilitation Engineering*, vol. 28, no. 7, pp. 1573-1583, July 2020, doi: 10.1109/TNSRE.2020.2989481.

[21] B. Shi *et al*., "Wearable ankle robots in post-stroke rehabilitation of gait: A systematic review," *Frontiers in neurorobotics*, vol. 13, no. 63, 2019.

[22] F. Hussain, R. Goecke, and M. Mohammadian, "Exoskeleton robots for lower limb assistance: A review of materials, actuation, and manufacturing methods," *Proceedings of the Institution of Mechanical Engineers, Part H: Journal of Engineering in Medicine*, vol. 235, no. 12, pp. 1375-1385, 2021.

[23] K. Batkuldinova, A. Abilgaziyev, E. Shehab, and M. H. Ali, "The recent development of 3D printing in developing lower-leg exoskeleton: A review," *Materials Today: Proceedings*, vol. 42, pp. 1822-1828, 2021.

[24] A. Aimar, A. Palermo, and B. Innocenti, "The role of 3D printing in medical applications: a state of the art," *Journal of healthcare engineering*, vol. 2019, 2019.

[25] J. Z. Gul *et al*., "3D printing for soft robotics–a review," *Science and technology of advanced materials*, vol. 19, no. 1, pp. 243-262, 2018.

[26] W. -Z. Li, G. -Z. Cao, and A. -B. Zhu, "Review on Control Strategies for Lower Limb Rehabilitation Exoskeletons," in *IEEE Access*, vol. 9, pp. 123040-123060, 2021, doi: 10.1109/ACCESS.2021.3110595.

[27] R. Kalra and M. Gupta, "A Review on Potential of Robotic Rehabilitation in Health Care System," *International Journal of Medical Science and Clinical Invention*, vol. 8, no. 5, pp. 5392–5413, May 2021, doi: 10.18535/ijmsci/v8i05.07.

[28] M. Dong *et al*., "A New Ankle Robotic System Enabling Whole-Stage Compliance Rehabilitation Training," *IEEE/ASME Transactions on Mechatronics*, vol. 26, no. 3, pp. 1490–1500, Jun. 2021, doi: 10.1109/TMECH.2020.3022165.

[29] S. Qu, R. Li, W. Yao, C. Ma, and Z. Guo, "Structure design, kinematics analysis, and effect evaluation of a novel ankle rehabilitation robot," *Applied Sciences*, vol. 13, no. 10, p. 6109, 2023.

[30] J. O. Akindoyo, M. D. Beg, S. Ghazali, H. P. Heim, and M. Feldmann, "Impact modified PLA-hydroxyapatite composites–Thermo-mechanical properties," *Composites Part A: Applied Science and Manufacturing*, vol. 107, pp. 326-333, 2018.

[31] M. A. M. Dzahir and S. I. Yamamoto, "Recent trends in lower-limb robotic rehabilitation orthosis: Control scheme and strategy for pneumatic muscle actuated gait trainers," *Robotics*, vol. 3, no. 2, pp. 120–148, Jun. 01, 2014.

[32] S. Hussain, "State-of-the-art robotic gait rehabilitation orthoses: Design and control aspects," *NeuroRehabilitation*, vol. 35, no. 4, pp. 701–709, Dec. 2014.

[33] M. Dong, J. Li, X. Rong, W. Fan, Y. Kong, and Y. Zhou, "Compliant physical interaction to enhance rehabilitation training of a parallel ankle robotic system," in *2020 Chinese Automation Congress (CAC)*, pp. 2191-2196, 2020.

[34] J. Li *et al*., "Mechanical Design and Performance Analysis of a Novel Parallel Robot for Ankle Rehabilitation," *Journal of Mechanisms and Robotics*, vol. 12, no. 5, Oct. 2020, doi: 10.1115/1.4046511.

[35] P. K. Jamwal, S. Hussain, Y. H. Tsoi, and S. Q. Xie, "Musculoskeletal Model for Path Generation and Modification of an Ankle Rehabilitation Robot," *IEEE Transactions on Human-Machine Systems*, vol. 50, no. 5, pp. 373–383, Oct. 2020, doi: 10.1109/THMS.2020.2989688.

[36] J. Li, W. Fan, M. Dong, and X. Rong, "Research on control strategies for ankle rehabilitation using parallel mechanism," *Cognitive Computation and Systems*, vol. 2, no. 3, pp. 105–111, Sep. 2020, doi: 10.1049/ccs.2020.0012.

[37] M. K. A. bin Ismail, M. N. Shah, and W. A. Mustafa, "Fabrication of Parallel Ankle Rehabilitation Robot," in *Lecture Notes in Mechanical Engineering*, pp. 623–637, 2021, doi: 10.1007/978-981-16-0866-7_53.

[38] M. Dong *et al*., "A New Ankle Robotic System Enabling Whole-Stage Compliance Rehabilitation Training," *IEEE/ASME Transactions on Mechatronics*, vol. 26, no. 3, pp. 1490–1500, Jun. 2021, doi: 10.1109/TMECH.2020.3022165.

[39] Francisco, J., & Fernandes, M. (n.d.). Study of the Influence of 3D Printing Parameters on the Mechanical Properties of PLA.

[40] I. Rojek, D. Mikołajewski, E. Dostatni, and M. Macko, "Ai-optimized technological aspects of the material used in 3d printing processes for selected medical applications," *Materials*, vol. 13, no. 23, pp. 1–19, 2020.

[41] A. J. van den Bogert, G. D. Smith, and B. M. Nigg, "In vivo determination of the anatomical axes of the ankle joint complex: An optimization approach," *J. Biomech*., vol. 27, no. 12, pp. 1477–1488, Dec. 1994.

[42] T. Alves, Q. Dong, J. Jacobson, C. Yablon, and G. Gandikota, "Normal and Injured Ankle Ligaments on Ultrasonography With Magnetic

Resonance Imaging Correlation," *Journal of Ultrasound in Medicine*, vol. 38, no. 2, pp. 513–528, 2019.

[43] A. A. Prakash, "Anatomy of Ankle Syndesmotic Ligaments: A Systematic Review of Cadaveric Studies," in *Foot and Ankle Specialist*, vol. 13, no. 4, pp. 341–350, 2020.

[44] P. Chauhan, A. K. Singh, and N. K. Raghuwanshi, "The state of art review on prosthetic feet and its significance to imitate the biomechanics of human ankle-foot," *Materials Today: Proceedings*, vol. 62, pp. 6364-6370, 2022.

[45] M. B. Ataoğlu, M. A. Tokgöz, A. Köktürk, Y. Ergişi, M. Y. Hatipoğlu, and U. Kanatlı, "Radiologic Evaluation of the Effect of Distal Tibiofibular Joint Anatomy on Arthroscopically Proven Ankle Instability," *Foot and Ankle International*, vol. 41, no. 2, pp. 223–228, 2020.

[46] C. Bergman, M. Morin, and K. Lawson, "Anatomy, Classification, and Management of Ankle Fractures Involving the Posterior Malleolar Fragment: A Literature Review," in *Foot and Ankle Orthopaedics*, vol. 4, no. 4, 2019.

[47] P. Faragó, L. Grama, M. A. Farago, and S. Hintea, "A novel wearable foot and ankle monitoring system for the assessment of gait biomechanics," *Applied Sciences*, vol. 11, no. 1, p. 268, 2020.

[48] C. Gao *et al*., "Comparative anatomy of the mouse and human ankle joint using Micro-CT: Utility of a mouse model to study human ankle sprains," *Mathematical Biosciences and Engineering*, vol. 16, no. 4, pp. 2959–2972, 2019.

[49] M. M. Gosselin, J. A. Haynes, J. J. McCormick, J. E. Johnson, and S. E. Klein, "The Arterial Anatomy of the Lateral Ligament Complex of the Ankle: A Cadaveric Study," *American Journal of Sports Medicine*, vol. 47, no. 1, pp. 138–143, 2019.

[50] C. Y. Hung, K. V. Chang, K. Mezian, O. Naňka, W. T. Wu, P. C. Hsu, and L. Özçakar, "Advanced ankle and foot sonoanatomy: imaging beyond the basics," *Diagnostics*, vol. 10, no. 3, p. 160, 2020.

[51] H. K. James, A. W. P. Chapman, V. Dhukaram, R. Wellings, and P. Abrahams, "Learning anatomy of the foot and ankle using sagittal plastinates: A prospective randomized educational trial," *Foot*, vol. 38, pp. 34–38, 2019.

[52] J. Jiang, K. M. Lee, and J. Ji, "Review of anatomy-based ankle–foot robotics for mind, motor and motion recovery following stroke: design considerations and needs," *International Journal of Intelligent Robotics and Applications*, vol. 2, no. 3, pp. 267–282, 2018.

[53] L. A. Lambert, L. Falconer, and L. Mason, "Ankle stability in ankle fracture," in *Journal of Clinical Orthopaedics and Trauma*, vol. 11, no. 3, pp. 375–379, 2020.

[54] K. A. Lawson, A. E. Ayala, M. L. Morin, L. D. Latt, and J. R. Wild, "Fracture-Dislocations: A Review," in *Foot and Ankle Orthopaedics*, vol. 3, no. 3, 2018.

[55] Y. Li, J. Ko, S. Zhang, C. N. Brown, and K. J. Simpson, "Biomechanics of ankle giving way: A case report of accidental ankle giving way during the drop landing test," *Journal of Sport and Health Science*, vol. 8, no. 5, pp. 494–502, 2019.

[56] R. L. Monteiro, C. D. Sartor, J. S. Ferreira, M. G. Dantas, S. A. Bus, and I. C. Sacco, "Protocol for evaluating the effects of a foot-ankle therapeutic exercise program on daily activity, foot-ankle functionality, and biomechanics in people with diabetic polyneuropathy: A randomized controlled trial," *BMC musculoskeletal disorders*, vol. 19, no. 1, pp. 1-12, 2018.

[57] C. Nery and D. Baumfeld, "Anterior and posterior ankle impingement syndromes: Arthroscopic and endoscopic anatomy and approaches to treatment," *Foot and ankle clinics*, vol. 26, no. 1, pp. 155-172, 2021.

[58] J. Vega, J. Karlsson, G. M. M. J. Kerkhoffs, and M. Dalmau-Pastor, "Ankle arthroscopy: the wave that's coming," *Knee Surgery, Sports Traumatology, Arthroscopy*, vol. 28, pp. 5-7, 2020.

[59] J. Vega, F. Malagelada, J. Karlsson, G. M. Kerkhoffs, M. Guelfi, and M. Dalmau-Pastor, "A step-by-step arthroscopic examination of the anterior ankle compartment," *Knee Surgery, Sports Traumatology, Arthroscopy*, vol. 28, no. 1, pp. 24–33, 2020.

[60] Y. Wang, Z. Li, D. W. C. Wong, C. K. Cheng, and M. Zhang, "Finite element analysis of biomechanical effects of total ankle arthroplasty on the foot," *Journal of Orthopaedic Translation*, vol. 12, pp. 55–65, 2018.

[61] Y. Wang, D. W. C. Wong, Q. Tan, Z. Li, and M. Zhang, "Total ankle arthroplasty and ankle arthrodesis affect the biomechanics of the inner foot differently," *Scientific Reports*, vol. 9, no. 1, 2019.

[62] M. B. Yandell, J. R. Tacca, and K. E. Zelik, "Design of a Low Profile, Unpowered Ankle Exoskeleton That Fits Under Clothes: Overcoming Practical Barriers to Widespread Societal Adoption," in *IEEE Transactions on Neural Systems and Rehabilitation Engineering*, vol. 27, no. 4, pp. 712-723, April 2019, doi: 10.1109/TNSRE.2019.2904924.

[63] S. Hall. *Basic biomechanics*. McGraw-Hill, Sixth Edition, 2012.

[64] A. Fomin, A. Antonov, V. Glazunov, and Y. Rodionov, "Inverse and forward kinematic analysis of a 6-dof parallel manipulator utilizing a circular guide," *Robotics*, vol. 10, no. 1, pp. 1–13, 2021.

[65] J. K. Mohanta, S. Mohan, P. Deepasundar, and R. Kiruba-Shankar, "Development and control of a new sitting-type lower limb rehabilitation robot," *Computers and Electrical Engineering*, vol. 67, pp. 330–347, 2018.

[66] A. Zubizarreta, M. Larrea, E. Irigoyen, I. Cabanes, and E. Portillo, "Real-time direct kinematic problem computation of the 3PRS robot using neural networks," *Neurocomputing*, vol. 271, pp. 104–114, 2018.

[67] N. S. Shalal and W. S. Aboud, "Smart robotic exoskeleton: A 3-dof for wrist-forearm rehabilitation," *Journal of Robotics and Control (JRC),* vol. 2, pp. 476-483, 2021.

[68] N. S. Shalal and W. S. Aboud, "Designing and Construction a Low-Cost Robotic Exoskeleton for Wrist Rehabilitation," *Journal of Mechanical Engineering Research and Developments*, vol 43, no. 4, pp. 180-192, 2020.

[69] J. C. Camargo, A. R. Machado, E. C. Almeida, and E. F. M. S. Silva, "Mechanical properties of PLA-graphene filament for FDM 3D printing," *International Journal of Advanced Manufacturing Technology*, vol. 103, pp. 2423–2443, 2019.

[70] S. A. Raj, E. Muthukumaran, and K. Jayakrishna, "A case study of 3D printed PLA and its mechanical properties," *Materials Today: Proceedings*, vol. 5, no. 5, pp. 11219-11226, 2018.

[71] T. Yao, Z. Deng, K. Zhang, and S. Li, "A method to predict the ultimate tensile strength of 3D printing polylactic acid (PLA) materials with different printing orientations," *Composites Part B: Engineering*, vol. 163, pp. 393-402, 2019.

[72] P. McKeown and M. D. Jones, "The Chemical Recycling of PLA: A Review," *Sustainable Chemistry*, vol. 1, no. 1, pp. 1–22, 2020.

[73] C. Valean, L. Maravina, M. Marghita, E. Linul, J. Razavi, F. Berto, and R. Brighenti, "The effect of crack insertion for FDM printed PLA materials on Mode I and Mode II fracture toughness," *Procedia Structural Integrity*, vol. 28, pp. 1134–1139, 2020.

[74] T. Yao, J. Ye, Z. Deng, K. Zhang, Y. Ma, and H. Ouyang, "Tensile failure strength and separation angle of FDM 3D printing PLA material: Experimental and theoretical analyses," *Composites Part B: Engineering*, vol. 188, p. 107894, 2020.

[75] Y. Zhao, Y. Chen, and Y. Zhou, "Novel mechanical models of tensile strength and elastic property of FDM AM PLA materials: Experimental and theoretical analyses," *Materials & Design*, vol. 181, p. 108089, 2019.

[76] A. M. E. Arefin, N. R. Khatri, N. Kulkarni, and P. F. Egan, "Polymer 3D Printing Review: Materials, Process, and Design Strategies for Medical Applications," *Polymers*, vol. 13, no. 9, p. 1499, 2021.

[77] D. F. Gordon, G. Henderson, and S. Vijayakumar, "Effectively quantifying the performance of lower-limb exoskeletons over a range of walking conditions," *Frontiers in Robotics and AI*, vol. 5, p. 61, 2018.

[78] K. E. Bijker, G. de Groot, and A. P. Hollander, "Differences in leg muscle activity during running and cycling in humans," *European Journal of Applied Physiology*, vol. 87, no. 6, pp. 556–561, 2002.

[79] A. G. Cresswell, W. N. Löscher, and A. Thorstensson, "Influence of gastrocnemius muscle length on triceps surae torque development and electromyographic activity in man," *Experimental brain research*, vol. 105, pp. 283-290, 1995.

[80] A. K. Mishra, A. Srivastava, R. P. Tewari, and R. Mathur, "EMG analysis of lower limb muscles for developing robotic exoskeleton orthotic device," *Procedia Engineering*, vol. 41, pp. 32–36, 2012.